DOI: https://doi.org/10.37434/tpwj2023.03.02

MATHEMATICAL MODELING OF RESIDUAL STRESSES IN A COMPOSITE WELDED JOINT OF THE COLLECTOR ADAPTER SLEEVE AND THE BRANCH PIPE OF PGV-440 STEAM GENERATOR

A.A. Makarenko[1], **O.V. Makhnenko**[2]

[1]STC of the E.O. Paton Electric Welding Institute of NASU
11 Kazymyr Malevych Str., 03150, Kyiv, Ukraine
[2]E.O. Paton Electric Welding Institute of the NASU
11 Kazymyr Malevych Str., 03150, Kyiv, Ukraine

ABSTRACT

Composite welded joints of dissimilar materials, usually steels of ferritic-pearlitic (bainitic) and austenitic grades, were used in elements of equipment and pipelines of operating nuclear power plants (NPP). The considerable difference in chemical composition of base material and welding consumables leads to chemical and structural heterogeneity of metal in the joint zone, and the difference in the coefficients of thermal expansion of the materials during welding and postweld heat treatment results in formation of high unrelaxed residual stresses, which significantly influence the strength, fatigue life and corrosion resistance of equipment elements. Considerable difficulties of experimental measurement of residual stresses make it complicated to take them into account at determination of the service life of nuclear power plant equipment elements. Damage of the Dn-1100 welded joint in the welded assembly of the coolant collector adapter sleeve from 08Kh18N10T stainless steel and the branch pipe of the steam generator body from 22K steel is one of the problems in safe operation of WWER-440 nuclear power units. Systematized information on the nature and causes for development of this damage are absent. In this connection, the methods of mathematical modeling were used to perform analysis of the microstructural phase composition and residual stresses, arising in this joint in welding, and of their influence on the service life of the welded assembly. Analysis of the results of mathematical modeling of the thermal processes, microstructural phase transformations and stress-strain state (SSS) in the composite welded joint showed that hardening structures in the HAZ of branch pipe metal (St22K) and lowering of the material crack resistance characteristics can be found at violation of surfacing and welding technology during steam generator manufacture, namely non-compliance with the conditions of preheating and concurrent heating ($T \geq 200$ °C). Rather high residual tensile stresses were determined on the composite joint inner surface, which is in contact with the coolant corrosive medium in operation, as well as in the zone of contact (fusion) of the material of branch pipe pearlitic steel with austenitic metal of the weld, where there is a high probability of discontinuity defect formation in welding. It may have a negative influence on the strength and structural integrity of the welded assembly of branch pipe of steam generator (SG) at further long-term service.

KEYWORDS: composite welded joint, PGV-440 steam generator, heat-affected zone, microstructural phase transformations, residual stresses, mathematical modeling

INTRODUCTION

Evaluation of strength, integrity and serviceability of welded joint components, which requires data on residual stresses, is one of the most important issues of safe operation and extension of service life of the equipment of nuclear power plants (NPP) of Ukraine. So-called composite welded joints (CWJ) of dissimilar materials, usually of steels of ferritic-pearlitic and austenitic grades, were quite often used in the elements of equipment and pipelines of operating NPP. A feature of the composite welded joints consists in that the difference in the chemical composition of the base metal and welding consumables may lead to considerable diffusion of chemical elements in the joint zone during welding heating, which causes chemical and structural heterogeneity of CWJ metal [1, 2]. In addition, considerable difference in the coefficients of thermal expansion of the component materials may give rise to significant unrelaxed residual stresses during welding and postweld heat treatment [3, 4]. Structural heterogeneity of CWJ metal and unrelaxed residual stresses have a noticeable influence on the strength, fatigue life and corrosion resistance of the equipment elements [5]. Considerable difficulties in experimental measurement of unrelaxed residual stresses make it more complicated to allow for them at determination of the service life of nuclear power plant equipment elements.

Starting from 2007, one of the problems for the operating nuclear power units of water-water energetic reactor 440 (WWER-440) is damage of CWJ Dn-1100 of the welded assembly of the coolant collectors from 08Kh18N10T stainless steel and branch pipe of the body of steam generators (SG) from 22K steel. The ring discontinuities (cracks) were detected in the zone of fusion of pearlitic and austenitic metals in power units of Armenian NPP, Dukovani NPP

Copyright © The Author(s)

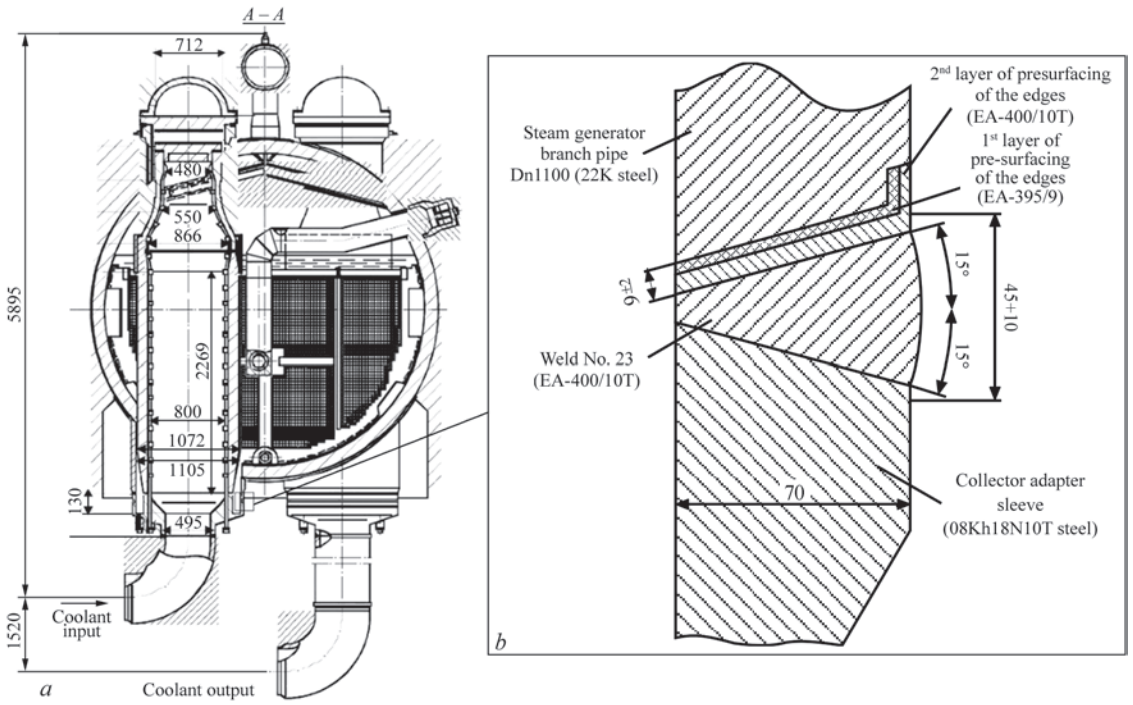

Figure 1. Design of PGV-440 with connected collectors (*a*) and schematic of welded joint of collector adapter sleeve and steam generator branch pipe (*b*)

(Czechia) and some others. Investigations of the nature and cause for development of a high damage level were conducted [13, 14]. Systematized information on analysis of residual stresses developing in this joint and their influence on welded assembly service life are absent.

DESIGN AND TECHNOLOGY OF MAKING THE CWJ OF SG BODY WITH THE COLLECTOR

Figure 1 shows the design of a welded joint in the welded assembly of the collector and branch pipe Dn-1100 of PGV-400 steam generator, which includes the following [6–8, 14]:

1. Steam generator branch pipe Dn-1100 from 22K steel with preliminary two-layer surfacing of the edge: first layer is EA-395/9 (Sv-10Kh16N25AM6), second layer is EA-400/10T (Sv-04Kh19N11MZ). Surfacing is performed with preheating to 100 °C with subsequent heat treatment by the mode of residual tempering at 640 + 20 °C with 9 h soaking.

2. Adapter sleeve from 08Kh18N10T steel, which has a tapered transition on external diameter, with variation of sleeve wall thickness from 70 mm (for welding to steam generator body branch pipe) to 35 mm (for welding the adapter sleeve to circulation pipeline).

3. Weld joining the adapter sleeve to steam generator branch pipe from 22K steel with presurfaced edge, which is made by manual electric-arc welding by EA-400/10T electrodes without preheating. No tempering to relieve the residual stresses is performed.

DAMAGEABILITY OF COMPOSITE WELDED JOINTS OF WWER-440 STEAM GENERATORS

The first damage in composite welded joints of WWER-440 steam generators was found at NPP [13] in 2007. In power unit No. 3 at operational control of metal of ZPG-1 seam generator inadmissible reflectors were detected by UT technique in welded joint No. 23kh (in SG, manufactured later, including those in Rivne NPP, welded joints No. 23kh and No. 23d are designated No. 76 and No. 77, respectively). Mechanical cutting out of templates from welded joint No. 23Kh was performed. Visual examination of the template showed a cracklike discontinuity, filled with corrosion products, which runs through the zone of fusion of pearlitic steel 22K with a deposit on the edge of weld No. 23Kh. The surface of the template from the side of steel 22K, which contacts the medium of the 2nd circuit, is affected by multiple general and pitting corrosion of up to ~3 mm depth.

The macrostructure of welded joint samples is given in Figure 2. Main cracks were detected in the macrosections, which have the same location and direction: from the weld root upwards through the fusion zone. In the sample, the transition deposit made with EA 395 electrode, is of nonuniform thickness, and a considerable part of the welded joint is absent (Figure 2, *a*).

Analysis of the results of fractographic studies on welded joint samples led to the following conclusions [14]:

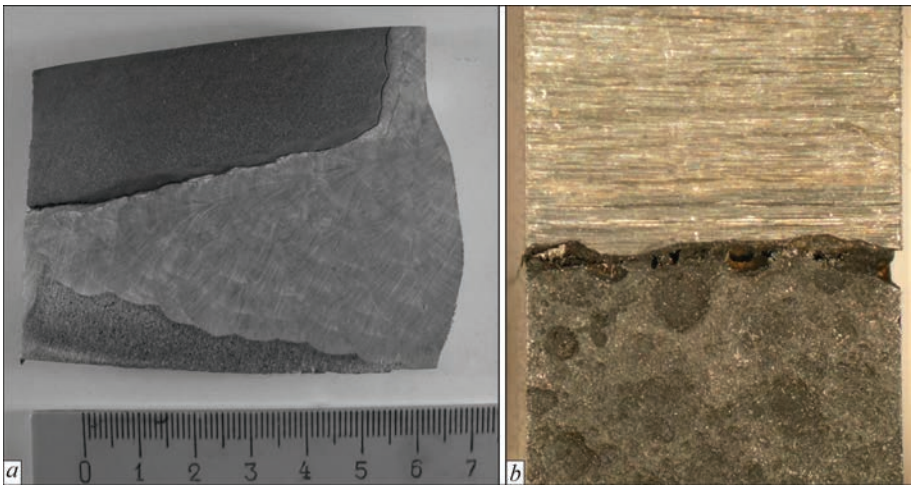

Figure 2. Macrostructure of the welded joint sample: *a* — cross-sectional view; *b* — view of the inner surface contacting the working medium of the 2nd circuit [14]

● main crack growth is staged and it is accompanied by intensive oxidation of its surface;

● the crack initiates in the zone of the fusion line of dissimilar materials of the composite welded joint, which is accompanied by intensive dissolution of base metal with development of a local corrosion center.

Thus, destruction is mainly of a corrosion-mechanical nature, and it can be indentified as stress corrosion cracking, due to a certain nature and level of the stress-strain state and simultaneous influence of the corrosive medium in the collector "pocket".

Moreover, in individual microzones of the sample metallographic analysis clearly established the presence of a changed layer, adjacent to the base metal [14]. This metal layer is the consequence of strong mixing of the metal of austenitic weld and carbon steel; its chemical composition has lower Cr and Ni content, which corresponds to the martensitic region of Scheffler phase diagram. The results of measurement of metal microhardness of the changed layer and of austenitic weld metal are indicative of the higher hardness of this layer, which is characteristic for martensite. Interlayers of acicular martensitic structure were revealed in the higher hardness layer, which could initiate cracking both right after manufacture and in service.

OBJECTIVE OF THE STUDY

Within the scope of solving the problems of safe operation of WWER-440 nuclear power units, mathematical modeling was performed of thermal processes, microstructural phase transformations and residual stresses in welding of composite welded joint Dn-1100 of the coolant collector adapter sleeve and branch pipe of the body of PGV-400 steam generator for further analysis of the nature and causes for damage, developing in this joint and their influence on the welded assembly service life.

DEVELOPMENT OF THE MATHEMATICAL MODEL OF SSS IN CWJ WELDING

Calculation-based prediction of residual stresses in the zone of CWJ of collector adapter sleeve and steam generator branch pipe Dn-1100 was performed using the methods of elasto-viscous-plastic analysis of the thermodeformational processes during surfacing of the steam generator branch pipe edge, intermediate heat treatment and filling the welded joint groove by multipass welding. Although it is believed that low-carbon pearlitic steel 22K is not prone to hardening structure formation under the impact of thermal cycles of welding, nonetheless modeling of microstructural phase transformations was conducted for a more detailed analysis of this matter. Modeling of the creep processes during intermediate heat treatment was performed after the edge surfacing, in order to determine the residual stress relaxation.

Taking into account the partially symmetric design of the welded assembly and the possibility of effective application of the assumption of fast-moving source of welding heat for modeling the temperature distributions and SSS of circumferential welded joints [9], a 2D finite-element model of the assembly of welded joint of the adapter sleeve and steam generator branch pipe Dn-1100 was plotted with the assumption of axial symmetry of the latter (Figure 1). The scheme of the model and boundary conditions of the welded assembly, and finite-element grid in the welded joint zone are shown in Figures 3–4.

The temperature problem was solved under the assumption of a fast-moving heat source, which allowed using a 2D finite-element model in the cross-section of the welded joint (Figure 2). Modeling of temperature distributions when making the welding passes was performed with application of the equation of

nonstationary heat conductivity, which includes allowing for a bulk welding heat source $W(x, y, t)$ [9]

$$\frac{\partial}{\partial x}\left(\lambda\frac{\partial T}{\partial x}\right)+\frac{\partial}{\partial y}\left(\lambda\frac{\partial T}{\partial y}\right)+ +W(x,y,t)=c\rho\frac{\partial T}{\partial t}, \quad (1)$$

where ρ is the material density; c is the specific heat conductivity; λ is the coefficient of heat conductivity; T is the material temperature.

$$W(x,y,t)=\frac{6Q}{ab\sqrt{\pi}}\times \times\exp\left(\frac{-3(x-x_0)^2}{a^2}-\frac{-3(y-y_0)^2}{b^2}\right), \quad (2)$$

where Q is the effective power of the welding heat source; x_0, y_0 are the coordinates of heat source center and a, b are the respective dimensions (width and depth) of the effective heating zone in x, y directions. The time of heating of the metal in each welding pass in the welded joint cross-section depends on welding speed v_w and size of effective heating zone a, in the first approximation, it may be equal to $t_w = a/v_w$.

The welding heat source parameters were selected so that the metal temperature in the weld did not exceed that of melting, and the time between the passes was sufficient for metal cooling to concurrent heating temperature.

Boundary conditions on the surfaces of welded joint elements, taking into account the convective heat exchange with the environment, were assigned in the following form:

$$q=-h(T_{out}-T), \quad (3)$$

where T_{out} is the ambient temperature; q is the heat flux; h is the coefficient of heat transfer from the surface at convective heat exchange with the environment.

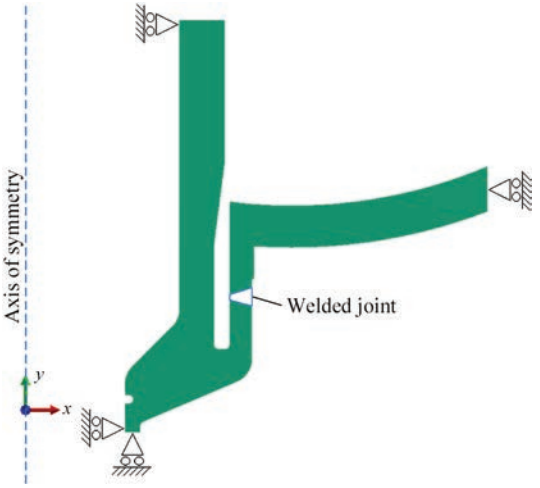

Figure 3. Scheme of 2D model (rotationally-symmetrical relative to axis *Y*) of welded joint assembly and boundary conditions

Nonstationary concentrated heating induces high temperature stresses, as well as plastic strains in the welded joint materials. Taking into account the "plane strain" hypothesis, solution of the problem on determination of the distribution of spatial components of stresses and strains was derived using a 2D model of the welded joint cross-section in the elastoplastic definition, i.e. this strain tensor can be presented as a sum of tensors:

$$\varepsilon_{ij}=\varepsilon_{ij}^e+\varepsilon_{ij}^p, \quad (i,j=x,y,z), \quad (4)$$

where ε_{ij}^e is the elastic strain tensor; ε_{ij}^p is the plastic strain tensor. The components of tensors of stresses σ_{ij} and elastic strains ε_{ij}^e are related to each other by the following Hooke's law:

$$\varepsilon_{ij}^e=\frac{\sigma_{ij}-\delta_{ij}\sigma}{2G}+\delta_{ij}(K\sigma+\varphi), \quad (5)$$

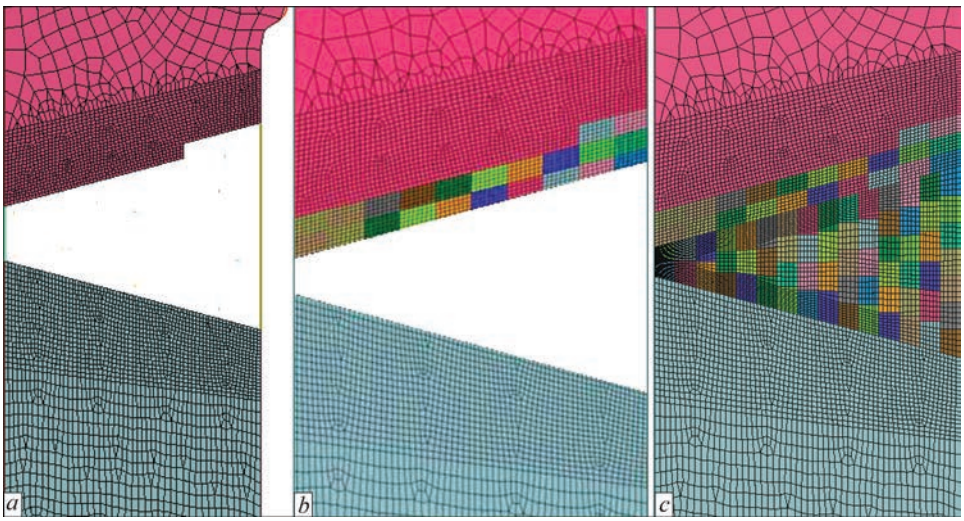

Figure 4. Finite-element grid in welded joint zone: *a* — before surfacing and welding; *b* — after edge surfacing; *c* — after welding

where δ_{ij} is the unit tensor ($\delta_{ij} = 0$, if $i \neq j$, $\delta_{ij} = 1$, if $i = j$); $\sigma = \frac{1}{3}(\sigma_{xx} + \sigma_{yy} + \sigma_{zz})$; $G = \frac{E}{2(1+\nu)}$ is the shear modulus; $K = \frac{1-2\nu}{E}$ is the bulk compression modulus; E is the Young's modulus; ν is the Poisson's ratio; φ is the function of free relative elongations (bulk changes), caused by the temperature change and microstructural phase changes. In a simple case, when no structural transformations take place:

$$\varphi = \alpha(T - T_0), \tag{6}$$

where α is the coefficient of relative temperature elongation of the material.

When welding steels, sensitive to the thermal cycle of welding, microstructural transformations with noticeable bulk changes can take place in the HAZ in K22 pearlitic steel for this welded joint. Allowing for them influences the kinetics of distribution of welding stresses and strains. The total effect of bulk changes from temperature T_0 up to $T(t)$ is found by [9]:

$$3\varphi = \frac{\sum V_j(T,t)\gamma_j(T) - \sum V_j(T_0)\gamma_j(T_0)}{\sum V_j(T_0)\gamma_j(T_0)}, \quad (j = m, b, fp, a), \tag{7}$$

where $\gamma_j(T)$ is the volume of a unit of mass of jth phase at temperature T, $V_j(T)$ is the fraction (in fractions of a unit) of jth phase at temperature T, m, b, fp, a indices are martensite, bainite, ferrite-pearlite and austenite, respectively.

Values $V_j(T)$ for low-alloyed steels can be determined, depending on carbon content C, % [15]:

$$\begin{aligned}
&\gamma_m(T) = 0.12282 + 8.56\cdot10^{-6}T + \\
&+ 2.15\cdot10^{-6}\,\text{C}, (\text{cm}^3/\text{g}); \\
&\gamma_a(T) = 0.12708 + 4.448\cdot10^{-6}T + \\
&+ 2.79\cdot10^{-6}\,\text{C}, (\text{cm}^3/\text{g}); \\
&\gamma_{b,fp}(T) = 0.12708 + 5.528\cdot10^{-6}T, (\text{cm}^3/\text{g});
\end{aligned} \tag{8}$$

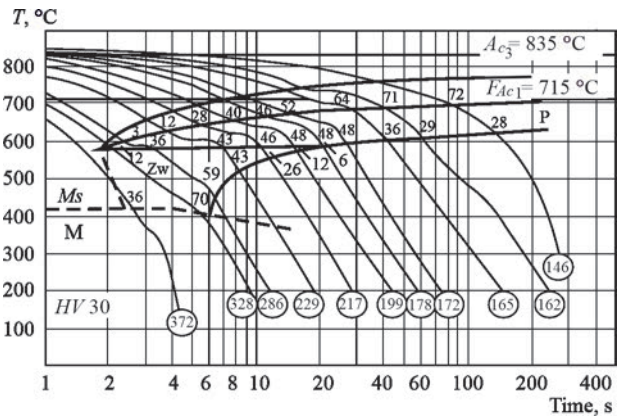

Figure 5. Thermokinetic diagram of austenite decomposition for melting steel close to 22K steel by its chemical composition (C 019 %, Si 0.294 % Mn 0.67 %, S 0.011%, P 0.074 %) [18]

Results of calculation of the mass fraction of each phase $V_j(T)$ in the final microstructure, depend on the cooling rate in the characteristic temperature range (rate of cooling from the temperature of 800 to 500 °C).

Kinetics of the changes of $V_j(T)$ value in the temperature range from $T_s^{(j)}$ — start of jth phase appearance up to $T_e^{(j)}$ — end of jth phase appearance at austenite decomposition, is defined from the following relationships:

$$\begin{aligned}
V_j(T) &= V_j^{\max}\left[1 - \exp\left(a_j \frac{T_{sj} - T}{T_{sj} - T_{ej}}\right)\right] \\
a_j &= -2,7 (j = m, fp, b); \\
V_a(T) &= 1 - \sum_{m,fp,b} V_j(T),
\end{aligned} \tag{9}$$

where $V_a(T)$ is the residual austenite content at temperature T.

Values of temperatures of the start $T_s^{(j)}$ and end $T_e^{(j)}$ of jth phase transformations, as well as its mass fraction in the final microstructure after cooling $V_j^{\max}$ for 22K steel were determined with application of parametric (regression) equations for low-alloyed steels, depending on their chemical composition and characteristic cooling time $\Delta t_{8/5}$, s (time of cooling from the temperature of 800 to 500 °C) [15, 16]:

$$\begin{aligned}
V_m^{\max} &= 0,5\left[1 - erf\frac{\ln \Delta t_{8/5} - \ln \Delta t_m^{50}}{\ln S_m}\right]; \\
V_{fp}^{\max} &= 0,5\left[1 + erf\frac{\ln \Delta t_{8/5} - \ln \Delta t_{fp}^{50}}{\ln S_{fp}}\right]; \\
V_b^{\max} &= 1 - V_m^{\max} - V_{fp}^{\max}.
\end{aligned} \tag{10}$$

Microstructural phase transformations were not modeled in 08Kh18N10T austenitic steel and EA-395/9 (Sv-10Kh16N25AM6), EA-400/10T (Sv-04Kh19N11M3) welding consumables.

A thermokinetic diagram of austenite decomposition (Figure 5) for producing steel [18], close by its composition (C 019 %, Si 0.294 %, Mn 0.67 %, S 0.011 %, P 0.074 %) was considered for analysis of the probable microstructural phase composition in the zone of edge surfacing and welding the branch pipe from 22K steel. One can see that at high cooling rates (30 % °C/s and higher) the branch pipe metal during edge surfacing by an austenitic material, or at subsequent multipass welding of the circumferential butt joint, a pearlitic-bainitic-martensitic structure forms with the possible maximum content of martensite of approximately up to 30 %.

Plastic strains are related to the stressed state by an equation of the theory of plastic nonisothermal flow, associated with von Mises yield criterion:

$$d\varepsilon_{ij}^{p} = d\lambda(\sigma_{ij} - \delta_{ij}\sigma), (i, j = x, y, z), \quad (11)$$

where $\partial\varepsilon_{ij}^{p}$ is the ε_{ij}^{p} tensor increment at the given moment of time t, due to the deformation history; stresses σ_{ij} and temperature T; $d\lambda$ is the scalar function, which is determined by flow conditions in the following form:

$$\begin{aligned} &d\lambda = 0, \text{ if } f = \sigma_i^2 - \sigma_y^2(T) < 0, \\ &\text{або } f = 0 \text{ at } df < 0; \\ &d\lambda > 0, \text{ if } f = 0 \text{ and } df > 0; \\ &f > 0 \text{ state is inadmissible,} \end{aligned} \quad (12)$$

where σ_i is the stress intensity.

$$\sigma_i = \frac{1}{\sqrt{2}} \times \sqrt{\left(\sigma_{xx} - \sigma_{yy}\right)^2 + \left(\sigma_{xx} - \sigma_{zz}\right)^2 + \left(\sigma_{yy} - \sigma_{zz}\right)^2 + 6\left(\sigma_{xy}^2 + \sigma_{xz}^2 + \sigma_{yz}^2\right)},$$

$\sigma_y(T)$ is the material yield limit at temperature T.

In order to obtain results on the components of residual stresses σ_{ij} and strains ε_{ij}, it is necessary to consider the process of development of elastoplastic strains in time, beginning from a certain initial state. The method of sequential tracking is traditionally used for this purpose, when for moment of time t the solution is sought, if complete solution for moment $(t - \Delta t)$ is known, where Δt is the step of tracking the development of elastoplastic strains, within which one can approximately assume that development proceeds by a rather simple loading path. In this case, the connection between the final increment of strain tensor $\Delta\varepsilon_{ij}$ and stress tensor σ_{ij} in keeping with [9], can be written in the following form:

$$\Delta\varepsilon_{ij} = \psi(\sigma_{ij} - \delta_{ij}\sigma) + \delta_{ij}(K\sigma) - b_{ij}, \quad (13)$$

where ψ is the function of material state in point (x, y, z) at moment t.

$$\begin{aligned} &\psi = \frac{1}{2G}, \text{ if } f < 0, \ \psi > \frac{1}{2G}, \text{ if } f > 0, \\ &\text{state } f > 0 \text{ is inadmissible,} \end{aligned} \quad (14)$$

b_{ij} is the tensor function of additional strains, which is determined by $\Delta\varphi$ increase and known results of the previous tacking stage:

$$b_{ij} = \left[\frac{\sigma_{ij} - \delta_{ij}\sigma}{2G} + \delta_{ij}(K\sigma)\right]_{t-\Delta t} + \delta_{ij}\Delta\varphi \quad (i, j = x, y, z). \quad (15)$$

Yield conditions in the form of (11) include significant physical nonlinearity in material state function ψ. Iteration processes are usually used for realization of this type of physical nonlinearity. As a result, in each iteration the physically nonlinear problem becomes a linear one of the type of a problem of the theory of elasticity with a variable shear modulus, which is equal to $1/2\psi$, and additional strains b_{ij}. Numerical methods are used for realization of such a linearized problem.

PHYSICOMECHANICAL PROPERTIES OF MATERIALS

Temperature fields at welding heating were calculated using the values of the coefficient of heat conductivity λ and bulk heat capacity ($c\rho$) of welded joint materials, depending on temperature (Figure 6, *a*, *b*). The deformation processes were calculated using the values of the temperature coefficient of linear expansion α, yield limit σ_y, modulus of elasticity E and Poisson's ratio ν of the materials, also depending on temperature (Figure 6, *c–f*). Dependencies of thermophysical and mechanical properties of the materials on temperature were derived according to reference books [16, 17], as well as by calculation by the chemical composition [19].

Most of the properties of 22K pearlitic steel (Figure 6, *a–d*) differ essentially from those of austenitic high-temperature steel 08Kh18N10T and EA-395/9 (Sv-10Kh16N25AM6), and EA-400/10T (Sv-04Kh19N11M3) welding consumables. Only the Young's modulus and Poisson's ratio are close by their values in the entire temperature range of heating (Figure 6 *e*, *f*).

DEVELOPMENT OF A MATHEMATICAL MODEL OF RESIDUAL STRESS RELAXATION AND REDISTRIBUTION DURING HEAT TREATMENT

In keeping with the data of certificates (PTD) [7, 8], when making composite welded joints of steam generator branch pipe Dn-1100 with the collector adapter sleeve after preliminary surfacing of the edge of the branch pipe from 22K steel by two layers of austenitic material, heat treatment was performed in the high-temperature tempering mode at 640 + 20 °C for 9 h. After making the welding passes of the joint of the adapter sleeve and the steam generator branch pipe with the preliminarily surfaced edge, no tempering was performed to relieve the residual stresses.

After performance of mathematical modeling of the heat treatment process after preliminary surfacing of the branch pipe edge, determination of the nonstationary temperature field was realized due to convective heat exchange on the surfaces at a gradual heating of the environment, soaking and further rather slow cooling. The nonstationary boundary conditions corresponded to uniform increase of ambient tempera-

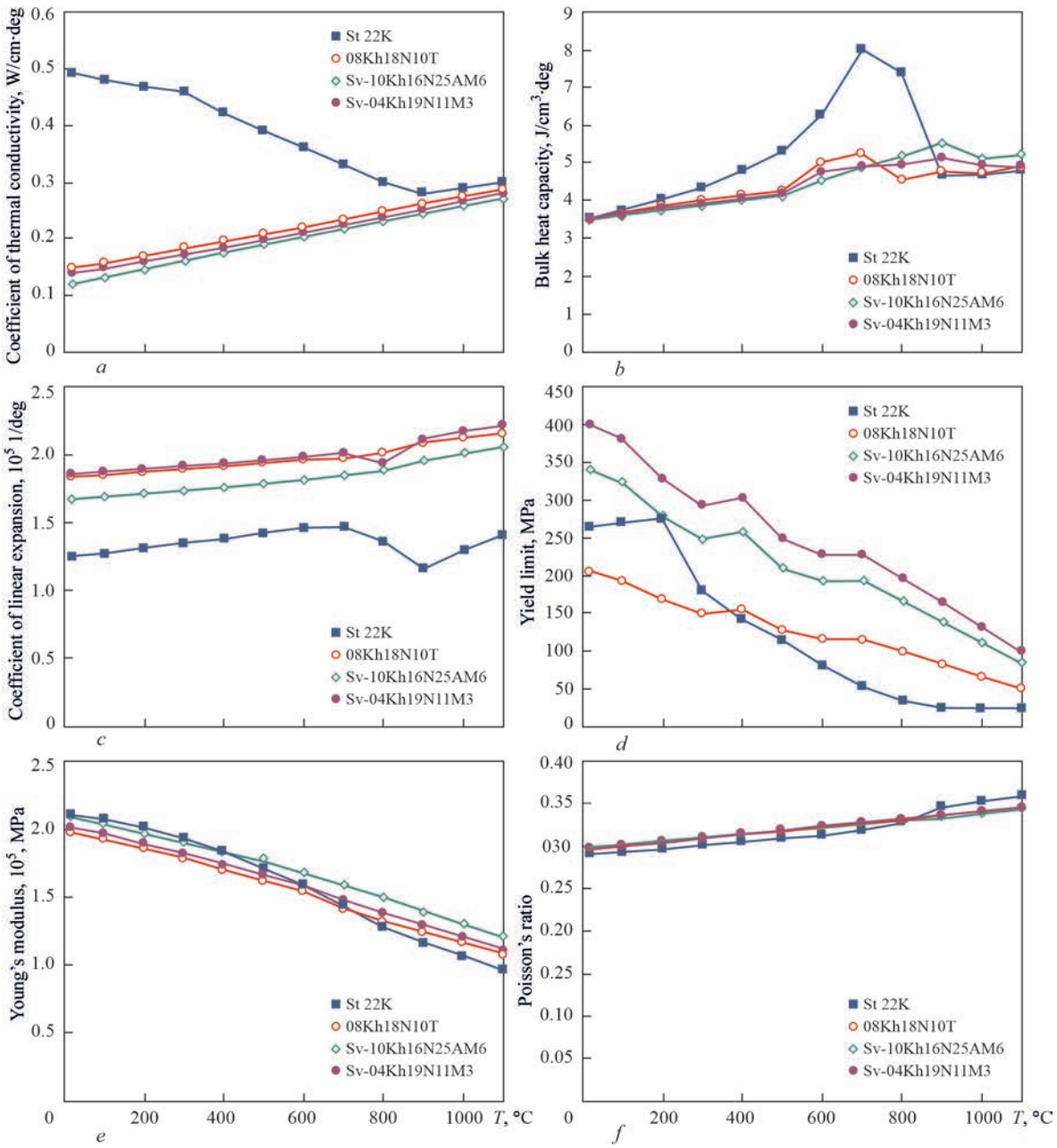

Figure 6. Mechanical and thermophysical properties of base materials: 22K steel, 08Kh18N10T steel and EA-395/9 (Sv-10Kh16N25AM6), EA-400/10T (Sv-04Kh19N11M3) welding consumables, depending on temperature [16–18]: *a* — coefficient of thermal conductivity; *b* — bulk heat capacity; *c* — coefficient of linear temperature expansion; *d* — yield limit; *e* — Young's modulus; *f* — Poisson's ratio

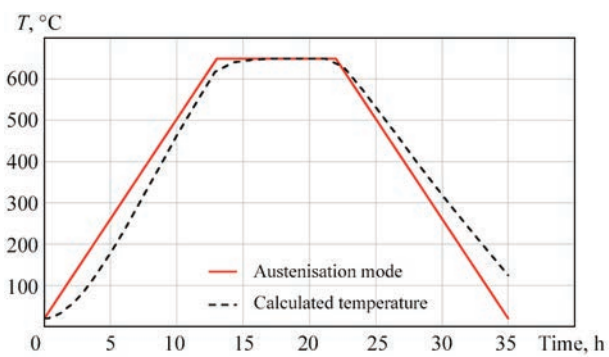

Figure 7. Graph of the change of the material temperature of branch pipe with surfaced edges during heat treatment

ture T_{amb} at the rate of 30 °C/h during heating up to 650 °C, soaking for 9 h and lowering to 20 °C at the rate of 30 °C/h at cooling (Figure 7).

The initial and boundary conditions of the boundary problem of determination of temperature distributions in the branch pipe with surfaced edges at heat treatment were as follows:

$$\text{at } t = 0,\ T_{out}(0) = 20\ ^\circ\text{C},\ T(0) = 20\ ^\circ\text{C},$$
$$q = -h(T_{out}(t) - T),$$
$$(T_{out}(t) = 30\ ^\circ\text{C/h}\cdot t,\ T_{out}^{\max} = 650\ ^\circ\text{C}.$$

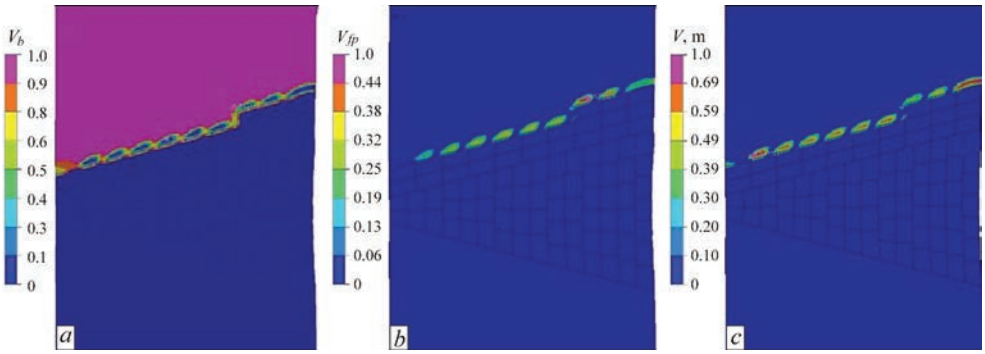

Figure 8. Results of modeling the residual microstructural composition in CWJ zone at $T_{preheating}$ = 100 °C; *a* — bainite; *b* — ferrite-pearlite; *c* — martensite

The coefficient of heat transfer from the branch pipe surface at convective heat exchange with the environment in the furnace and in air was taken equal to value h = 30 W/m^2 under the conditions of natural convection and heating and cooling constant in the entire range of heating and cooling temperatures. Radiant heat exchange in the developed model was not modeled separately, and its contribution was taken into account in a certain increase of the value of heat transfer coefficient.

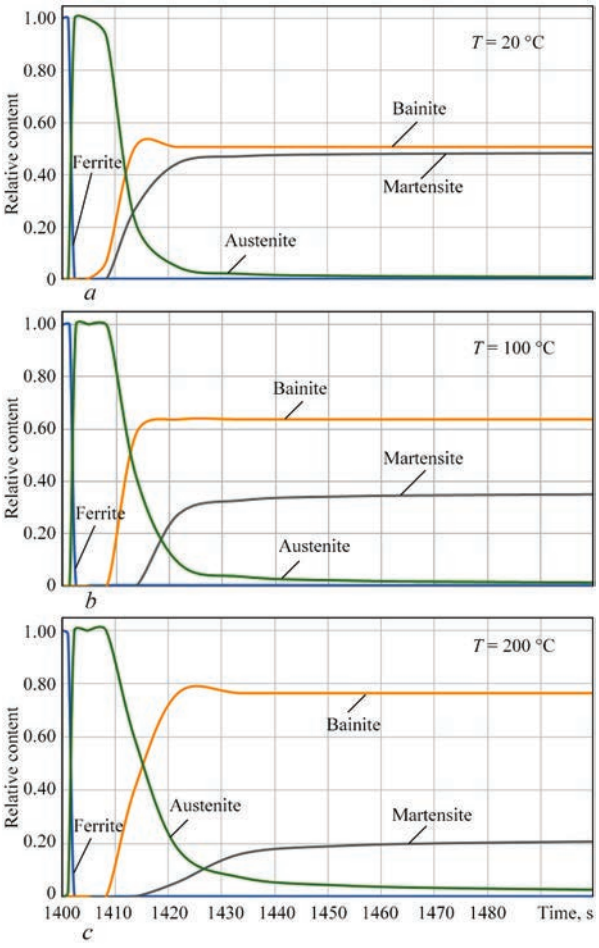

Figure 9. Kinetics of microstructural phase transformations in the characteristic point of the HAZ of SG branch pipe base material (22K steel) for different preheating temperatures: *a* — without preheating; *b* — $T_{preheating}$ = 100 °C; *c* – $T_{preheating}$ = 200 °C

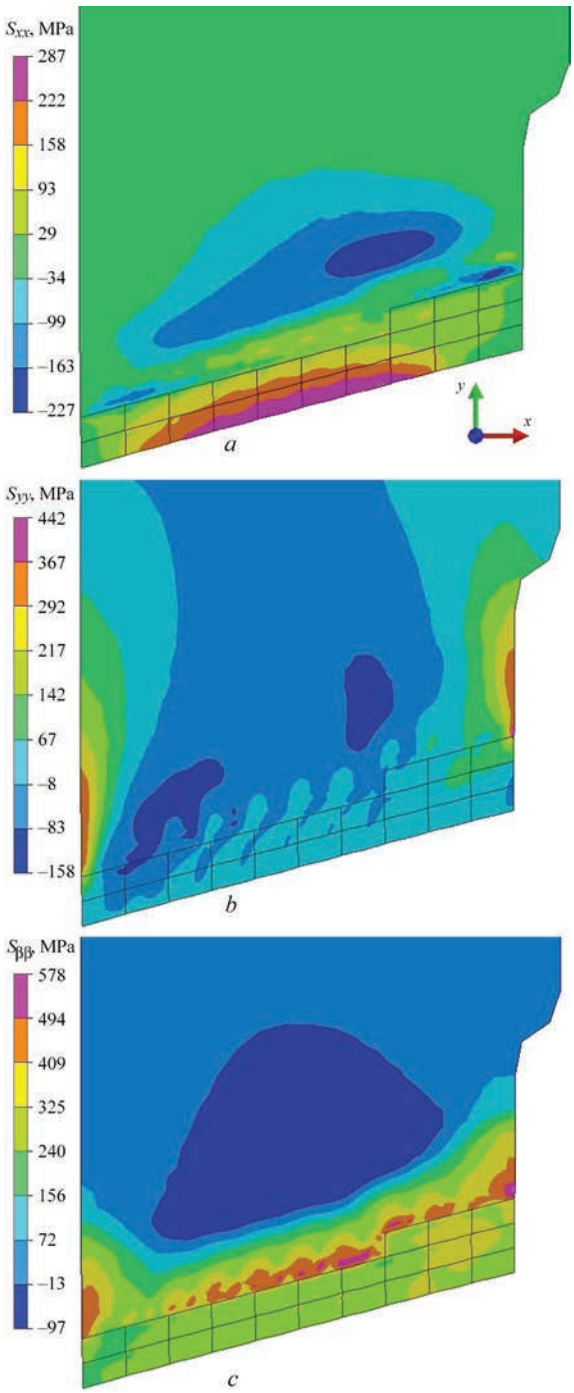

Figure 10. Residual stresses after surfacing the of SG branch pipe edges: *a* — radial σ_{xx}; *b* — axial σ_{yy} ; *c* — circumferential $\sigma_{\beta\beta}$

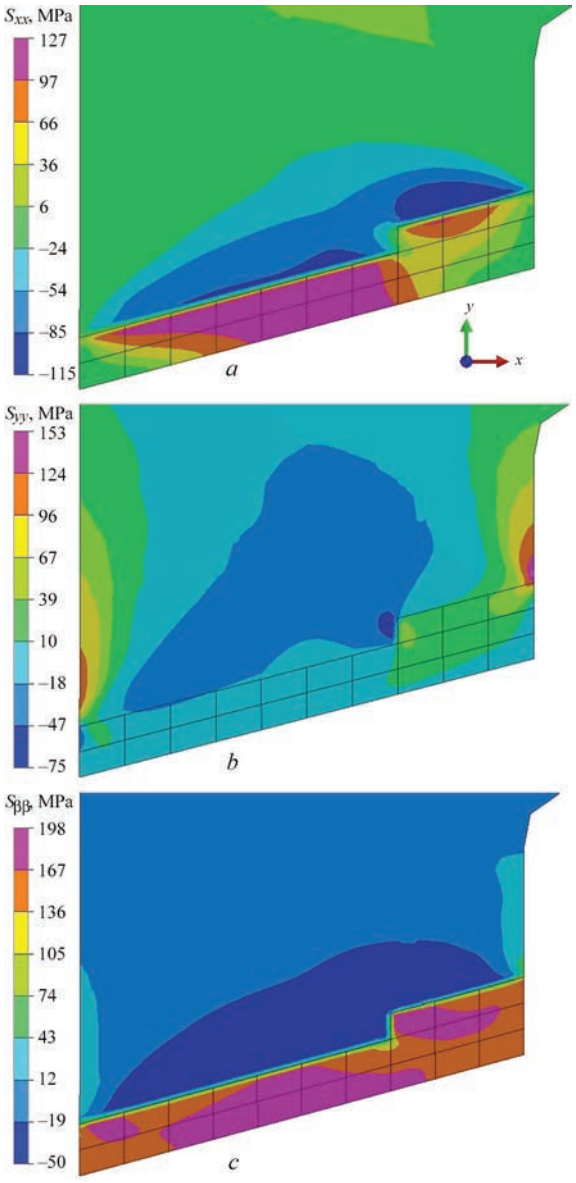

Figure 11. Residual stresses after heat treatment of SG branch pipe edge (T = 650 °C, $T_{soaking}$ = 9 h): *a* — radial σ_{xx}; *b* — axial σ_{yy}; *c* — circumferential $\sigma_{\beta\beta}$

The long-term process of heating up to the soaking temperature of 650 °C causes the processes of high-temperature creep in the material of the branch pipe and the austenitic deposit, which leads to relaxation and redistribution of residual stresses in the surfacing zone.

In the developed model the problem of determination of SSS at heat treatment was solved in the visco-elastoplastic definition [9]:

$$\varepsilon_{ij} = \varepsilon_{ij}^{e} + \varepsilon_{ij}^{p} + \varepsilon_{ij}^{cr} \ (i, j = x, y, z), \tag{16}$$

where the creep strain rate was determined by Bailey–Norton law [11]:

$$\dot{\varepsilon}_{ij}^{cr} = A\sigma_{eq}^{n}. \tag{17}$$

For 22K steel of pearlitic grade at the temperature of 650 °C the following coefficients can be taken, when determining the temperature creep strain rate: $A = 1.73 \cdot 10^{-14}$, $n = 5$ [9], and for austenitic materials of deposits on the edges of SG branch pipe $A = 6.948 \cdot 10^{-14}$, $n = 6.22$ [12].

RESULTS OF MATHEMATICAL MODELING OF TEMPERATURE DISTRIBUTIONS AND MICROSTRUCTURAL PHASE TRANSFORMATIONS

Results of modeling the microstructural transformations in CWJ metal during welding heating ($T_{preheating}$ = = 100 °C) and further cooling revealed (Figure 8) local formation of hardening structures in the HAZ of SG branch pipe metal (22K steel). Figure 9 shows the graphs of the change of microstructural phase state in the characteristic point of SG base material HAZ during welding and further cooing, where maximal residual content of martensite was obtained for different values of the preheating temperature. Application of preheating on the level of T = 200 °C in CWJ welding allows lowering the maximal relative content of martensite in the HAZ from 50 to 20 %, compared to welding without preheating.

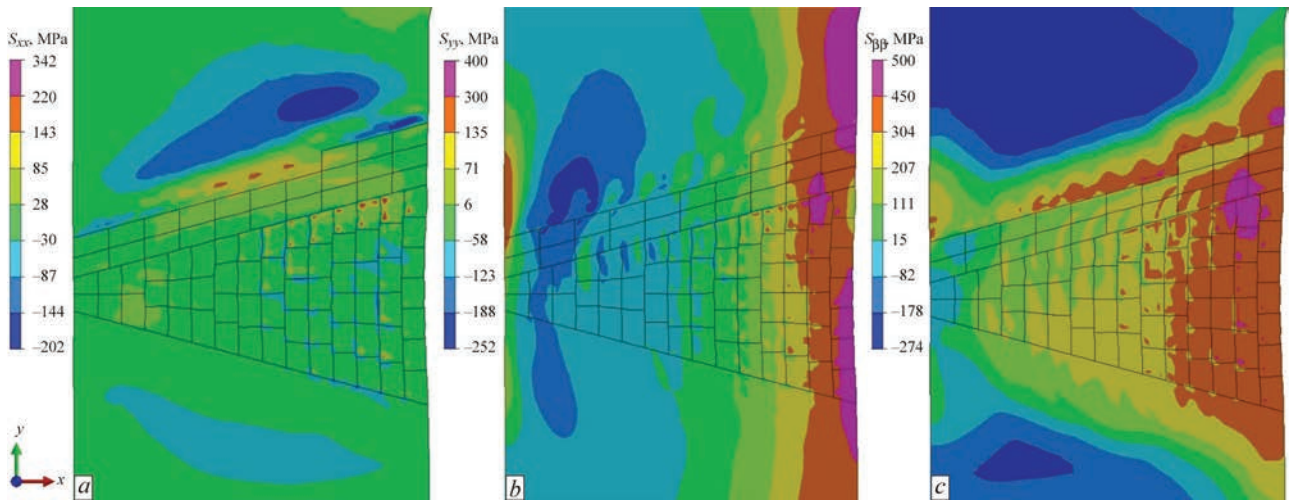

Figure 12. Residual stresses in CWJ after welding: *a* — radial σ_{xx}; *b* — axial σ_{yy}; *c* — circumferential $\sigma_{\beta\beta}$

RESULTS OF MATHEMATICAL MODELING OF RESIDUAL STRESSES AFTER WELDING AND AFTER HEAT TREATMENT

Figure 10 shows the distributions of residual stresses after surfacing the edge of SG branch pipe CWJ at the temperature of preheating and concurrent heating $T_{preheating}$ = 100 °C and subsequent cooling to T = 20 °C. The radial component (Figure 10, *a*) is characterized by a low level of stresses and local zones of maximum tensile stresses of up to 250 MPa in the austenitic material of the deposit. The axial (relative to branch pipe axis) component (Figure 10, *b*) is also characterized by the general low level of stresses and local zones of maximal tensile stresses of up to 300 MPa in the base material of SG branch pipe, which is adjacent to the austenitic weld metal on the inner and outer surfaces of the branch pipe. For the circular component of residual stresses (Figure 10, *c*) the tensile stresses (up to 400 MPa) were determined in the zone of SG branch pipe base material, adjacent to the austenitic weld metal.

After heat treatment (T = 650 °C, $T_{soaking}$ = 9 h) the level of residual stresses induced by surfacing the SG branch pipe edges decreases considerably: maximal radial tensile stresses are up to 120 MPa (Figure 11, *a*), axial ones are up to 130 MPa (Figure 11, *b*), circumferential stresses are up to 190 MPa (Figure 11, *c*).

After multipass welding performance very nonuniform distributions of residual stresses were obtained. The radial component in the welded joint zone (Figure 12, *a*) is characterized by a low level of stresses and local zones of maximal tensile stresses of up to 140 MPa in the base material of SG branch pipe, adjacent to the austenitic weld metal. Axial residual stresses (Figure 12, *b*) have a local zone of maximal tensile stresses

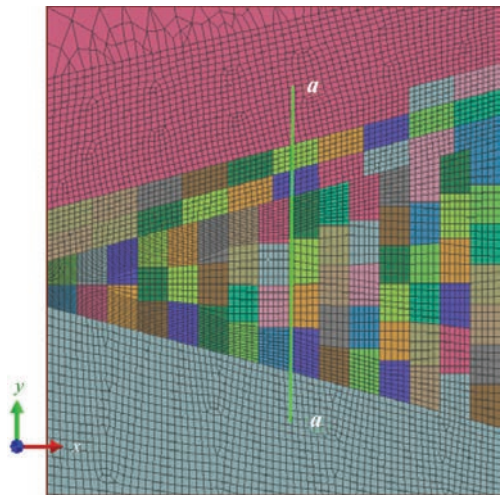

Figure 13. Welded joint section for determination of characteristic stress distributions

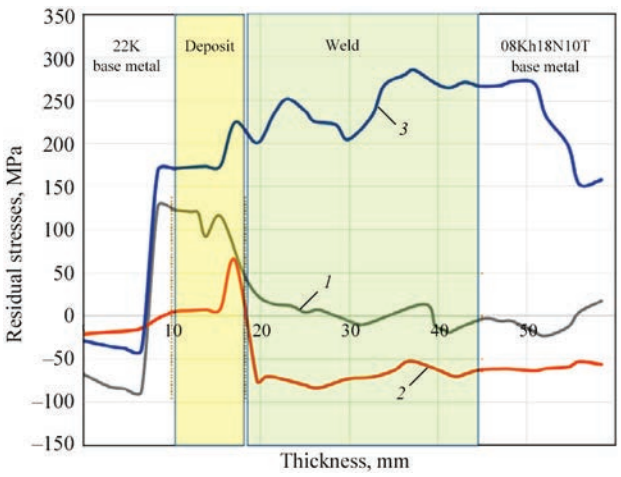

Figure 14. Residual stress distribution in the middle section (*a–a* in Figure 13) of the welded joint: *a* —radial σ_{xx}; *b* — axial σ_{yy}; *c* — circumferential $\sigma_{\beta\beta}$

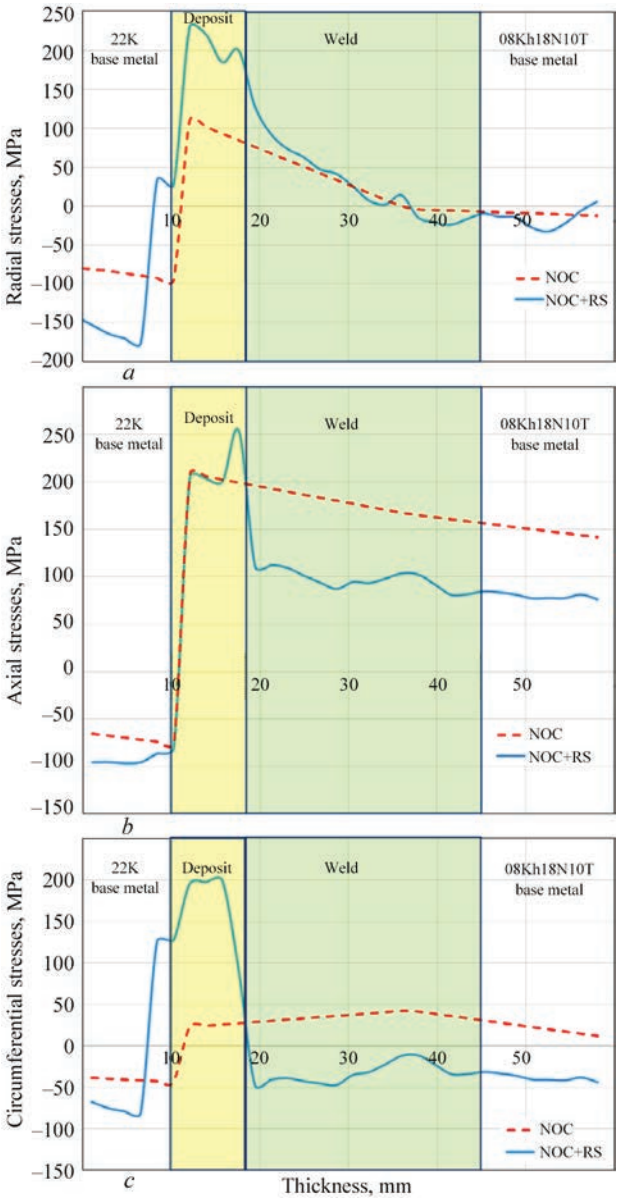

Figure 15. Distributions of operational stresses (operational at NOC, as well as summary operational and residual stresses) in the middle section (*a–a* in Figure 13) of the welded joint: *a* — radial σ_{xx}; *b* — axial σ_{yy}; *c* — circumferential $\sigma_{\beta\beta}$

of up to 200 MPa on the joint inner surface in the base material of SG branch pipe, adjacent to the austenitic weld metal, and tensile stresses of up to 400 MPa are found on the joint outer surface. The highest tensile stresses (up to 450 MPa) were determined for the circular component of the residual stresses (Figure 12, *c*) in the zone of base material of SG branch pipe, adjacent to austenitic weld metal, as well as in the weld material closer to the joint outer surface.

Thus, modeling of CWJ welding showed rather high residual tensile stresses. It is particularly dangerous on the joint inner surface, which is in contact with the coolant corrosive medium in service, as well as in the zone of contact (fusion) of the branch pipe material, namely of pearlitic grade steel with the austenitic metal of the deposit (weld). In this zone there is a high probability of discontinuity defect formation in welding, which may have a negative effect on SG strength at further long-term service.

The graphs of distribution of residual stresses (Figure 14) and operational stresses (operational at normal operating conditions (NOC), as well as summary operational and residual stresses) (Figure 15) in the welded joint middle section (*a–a* in Figure 13) of the welded joint were plotted. The influence of residual stresses (RS) on the stressed state of CWJ assembly is quite significant, namely, in the zone of surfacing and contact (fusion) of the material of branch pipe pearlitic steel to the austenitic metal of the deposit, a noticeable increase in the total stresses takes place, compared to the operational stresses, without allowing for residual stresses (Figure 15, *a*, *c*).

CONCLUSIONS

Analysis of the results of mathematical modeling of the thermal processes, microstructural phase transformations and SSS in the composite welded joint of the collector and the adapter sleeve of PGV-440 steam generator showed that:

1. In welding without preheating, the residual content of hardening structures in the HAZ of branch pipe metal (St22K) can reach 65 %. Application of preliminary (concurrent) preheating ($T \geq 200$ °C) allows a significant lowering of the relative content of martensite in the base material on the fusion boundary with austenitic material of the weld. However, considering the possible violations of the surfacing and welding technology at steam generator manufacture, we should assume the presence of hardening structures in the HAZ of branch pipe metal and lowering of the material crack resistance characteristics.

2. Failure to perform the final postweld heat treatment leads to formation of a complex pattern of distribution of residual stresses with high tensile stresses, both in the zone of the pearlitic material of the branch pipe, and in the zones of austenitic materials of the weld and the collector adapter sleeve.

3. Rather high residual tensile stresses were determined on the inner surface of the composite joint, which during operation is in contact with the coolant corrosive medium, as well as in the zone of fusion of the material of branch pipe pearlitic steel and austenitic metal of the weld, where there is a rather high probability of discontinuity defect formation in welding, which may have a negative influence of the strength and structural integrity of SG welded assembly at further long-term service.

REFERENCES

1. Makhnenko, V.I., Saprykina, G.Yu. (2002) Role of mathematical modeling in solving problems of welding dissimilar steels (Review). *The Paton Welding J*., **3**, 14–25.
2. Makhnenko, V.I., Kozlitina, S.S., Dzyubak, L.I. et al. (2010) Risk of formation of carbides and α-phase in welding of high-alloy chrome-nickel steels. *The Paton Welding J*., **12**, 5–8.
3. Wenchun, J., Wanchuck, W., Yun, L. et al. (2017) Residual stress distribution in a dissimilar weld joint by experimental and simulation study. ***J.*** *of Pressure Vessel Technology*, **139**, 011422-1-011422-10.
4. Deng, D., Ogawa, K., Kiyoshima, S. et al. (2009) Prediction of residual stresses in a dissimilar metal welded pipe with considering cladding, buttering and post weld heat treatment. *Computational Material Sci*., **47**, 398–408.
5. Kasatkin, O.G., Tsaryuk, A.K., Skulsky, V.Yu. et al. (2007) Method for improving local damage resistance of welded joints in NPP pipelines. *The Paton Welding J*., **3**, 27–30.
6. *Steam generator PGV-213*: Operating manual U 213-I-553 [in Russian].
7. *Steam generator body*: Certificate. 1137.50.06.000 PS [in Russian].
8. *Steam generator body*: Certificate. 1137.50.07.000 PS [in Russian].
9. Makhnenko, V.I. (2006) *Safe service life of welded joints and assemblies of modern structures*. Kyiv, Naukova Dumka [in Russian].
10. SOU NAEK 159E: *Safe operation. Welding and surfacing of equipment and pipelines of nuclear power plants with WWER reactors* [in Russian].
11. Rabotnov, Yu.N. (1966) *Creep of structure elements*. Moscow, GIFML [in Russian].
12. Margolin, B.Z., Gulenko, A.G., Kursevich, I.P. et al. (2006) Modeling for fracture in materials under long-term static creep loading and neutron irradiation. Pt 2. Prediction of creep rupture strength for austenitic materials. *Strength of Materials*, 38(**5**), 449–457.
13. Khodakov, V.D., Kharina, I.D., Korneev, A.E. (2008) Examination of nature and damage causes of dissimilar welded joints in welding of transition ring to branch pipe Dn1100 assembly at Novovoronezhsky and Kolsky NPP. In: *Proc. of 10th Int. Conf. (St.-Petersburg, October 2008)*. Vol. 2, St.-Petersburg, Prometej.
14. Vardanyan, A.M. ((2017) *Evaluation of influence of service conditions on residual life of assemblies of steam generators of power units WWER-440*: Syn. of Thesis for Cand. of Tech. Sci. Degree. Erevan, NPUA [in Russian].
15. Kasatkin, O.G., Seyffarth, P. (2002) Calculation models for evaluation of mechanical properties of HAZ metal in welding of low-alloyed steels. In: *Proc. of Int. Conf. on Mathematical*

Modeling and Information Technologies in Welding and Related Processes. Kyiv, 103–106.
16. (2003) *Steel and alloy grades*. Ed. by A.S. Zubchenko. Moscow, Mashinostroenie [in Russian].
17. (2003) *Mechanical properties of structural materials in complex stress state.* Ed. by A.A. Lebedev. Kyiv, In Yure [in Russian].
18. Seyfarth, Meyer, Scharf (1992) Großer Atlas Schweiß-ZTU-Schaubilder *Fachbuchreihe Schweißtechnik*, **110**. Düsseldorf, DVS Verlag.
19. Saunders, N., Guo, U.K., Li, X. et al. (2003). Using JMatPro to model materials properties and behavior. *JOM*, **55**, 60–65. DOI: https://doi.org/10.1007/s11837-003-0013-2

ORCID
A.A. Makarenko: 0000-0002-4713-9726,
O.V. Makhnenko: 0000-0002-8583-0163

CONFLICT OF INTEREST
The Authors declare no conflict of interest

CORRESPONDING AUTHOR
O.V. Makhnenko
E.O. Paton Electric Welding Institute of the NASU
11 Kazymyr Malevych Str., 03150, Kyiv, Ukraine.
E-mail: makhnenko@paton.kiev.ua

SUGGESTED CITATION
A.A. Makarenko, O.V. Makhnenko (2023) Mathematical modeling of residual stresses in a composite welded joint of the collector adapter sleeve and the branch pipe of PGV-440 steam generator. *The Paton Welding J.*, **3**, 8–19.

JOURNAL HOME PAGE
https://patonpublishinghouse.com/eng/journals/tpwj

Received: 08.03.2023
Accepted: 24.04.2023

SUBSCRIPTION–2023

«The Paton Welding Journal» is Published Monthly Since 2000 in English, ISSN 0957-798X, doi.org/10.37434/tpwj.

«The Paton Welding Journal» can be also subscribed worldwide from catalogues subscription agency EBSCO.

If You are interested in making subscription directly via Editorial Board, fill, please, the coupon and send application by Fax or E-mail.

12 issues per year, back issues available.

$384, subscriptions for the printed (hard copy) version, air postage and packaging included.

$312, subscriptions for the electronic version (sending issues of Journal in pdf format or providing access to IP addresses).

Institutions with current subscriptions on printed version can purchase online access to the electronic versions of any back issues that they have not subscribed to. Issues of the Journal (more than two years old) are available at a substantially reduced price.

The archives for 2009–2021 are free of charge on www://patonpublishinghouse.com/eng/journals/tpwj

ADVERTISING
in «The Paton Welding Journal»

External cover, fully-colored:
First page of cover
(200×200 mm) — $700
Second page of cover
(200×290 mm) — $550
Third page of cover
(200×290 mm) — $500
Fourth page of cover
(200×290 mm) — $600

Internal cover, fully-colored:
First/second/third/fourth page
(200×290 mm) — $400

Internal insert:
(200×290 mm) — $340
(400×290 mm) — $500

- Article in the form of advertising is 50 % of the cost of advertising area
- When the sum of advertising contracts exceeds $1001, a flexible system of discounts is envisaged
- Size of Journal after cutting is 200×290 mm

Address
11 Kazymyr Malevych Str., 03150, Kyiv, Ukraine
Tel./Fax: (38044) 205 23 90
E-mail: journal@paton.kiev.ua
www://patonpublishinghouse.com/eng/journals/tpwj